

# Neural Network Research on Validating Experimental Tilt-Rotor Performance



Sesi Kottapalli

*Aeromechanics Branch, Army/NASA Rotorcraft Division  
NASA Ames Research Center, Moffett Field, CA*

Results from a neural network study to validate full-scale XV-15 tilt-rotor experimental hover and forward flight data are presented. In the context of the present study, neural-network-based test data validation includes the following: test data representation, test data quality assessment (e.g., isolating "bad" test points), and finally, for outdoor hover measurements, wind correction procedure development. Two test databases, acquired during separate tests conducted at NASA Ames, were used. These two isolated XV-15 rotor test databases were obtained from tests in the 80- by 120-Foot Wind Tunnel and an outdoor hover test facility. Neural networks were successfully used to represent and assess the quality of full-scale tilt-rotor hover and forward flight performance test data. The neural networks accurately captured tilt-rotor performance at steady operating conditions and it was shown that the wind tunnel forward flight performance test data were generally of very high quality. Compared to existing momentum-theory based wind corrections to outdoor hover performance, the present neural-network-procedure-based corrections were better. The present wind corrections procedure, based on a well-trained neural network, captured physical trends present in the outdoor hover test data that had been missed by the existing momentum-theory method.

## Nomenclature

A	rotor disc area, $\pi R^2$ , m <sup>2</sup>
$C_Q$	rotor torque coefficient, torque/ $\rho ARV_{tip}^2$
$C_{QCORRM}$	rotor torque coefficient, corrected using momentum theory, Eq. 1
$C_T$	rotor thrust coefficient, thrust/ $\rho AV_{tip}^2$
$C_Y$	rotor side force coefficient, Side force/ $\rho AV_{tip}^2$
FM	figure of merit, $FM = 0.707C_T^{3/2}/C_Q$
$FM_{CORRNN}$	figure of merit, corrected using neural-network-based procedure, Eq. 4
$FM_{TEST}$	figure of merit, test
$FM_{ZW}$	neural network representation of figure of merit data where the wind is less than 0.5 m/s
$M_{tip}$	blade tip Mach number
MIMO	multiple-input, multiple-output
MISO	multiple-input, single-output
R	rotor radius, m
SIMO	single-input, multiple-output
SISO	single-input, single-output
V	wind tunnel airspeed
$V_h$	ideal induced hover velocity, $V_{tip} (C_T/2)^{1/2}$ , m/s
$V_i$	ideal induced velocity, m/s
$V_{tip}$	blade tip speed, $\Omega R$ , m/s
$V_w$	wind speed, m/s
$\alpha_s$	rotor shaft angle, positive nose up, deg

$\Delta_T$	figure of merit delta, difference between test and zero wind figures of merit, Eq. 3
$\Delta_{TNN}$	figure of merit delta predicted by neural network
$\Theta_0$	collective angle, deg
$\lambda_h$	ideal induced hover velocity ratio, $V_h/V_{tip}$
$\lambda_i$	ideal induced velocity ratio, $V_i/V_{tip}$
$\mu$	rotor advance ratio, $V \cos \alpha_s / (\Omega R)$
$\mu_x$	axial component of outdoor wind velocity ratio, $(V_w \cos \psi_w)/V_{tip}$ , positive into rotor disk when viewed from above (direction opposite to thrust direction)
$\mu_y$	lateral component of outdoor wind velocity ratio, $(-V_w \sin \psi_w)/V_{tip}$ , positive towards right when viewed from above (direction same as side force direction)
$\sigma$	rotor solidity ratio
$\psi_w$	wind direction relative to rotor axis
$\Omega$	rotor rotation speed, rad/sec

## Introduction

The advantages of rotorcraft wind tunnel testing include cost and safety benefits, as the rotorcraft model is rigorously evaluated prior to its first flight test. By allowing significant operational variations to be systematically introduced into the test conditions, wind tunnel tests of experimental models provide valuable data. Further, these wind tunnel test conditions can be well outside the flight envelope. Thus, a wind tunnel test can encompass a larger test envelope compared to a flight test, making wind tunnel testing indispensable.

Rotorcraft aerodynamic performance measurement and prediction involve a high a level of complexity, and it is difficult at times to even heuristically know the variation of the test data with changes in operating

Based on a paper presented at the 16th AIAA Applied Aerodynamics Conference, Albuquerque, New Mexico, June 1998. Manuscript received November 1998; accepted February 2000.

conditions. Since the test data trends may be new and without precedent, it becomes difficult to expeditiously isolate "bad" data points from the "good" points. As such, it is more difficult to interpret the quality of the measured data and the trends projected by wind tunnel tests. For outdoor hover testing, the influence of outdoor winds has to be properly corrected when analyzing the test data. Thus, there is a need for a consistent, easy-to-understand and easy-to-apply process for evaluating and correcting data obtained from wind tunnel and hover facility tests.

This paper presents results from a neural network study conducted to validate full-scale experimental tilt-rotor performance data. These experimental performance data include data obtained from a wind tunnel test facility and from an outdoor hover test facility. The outdoor performance data need to be "wind-corrected" to obtain the correct tilt-rotor hover performance characteristics. In the present study, the use of neural networks is justified because of their multi-dimensional, nonlinear curve fitting characteristics. The present work is considered to be a generic methodology and is not specific to the presently considered tilt-rotor configuration. Neural network studies on rotorcraft dynamics were initiated in the Army/NASA Rotorcraft Division at NASA Ames Research Center, as discussed in Refs. 1-4. The experience gained from these neural network studies was very useful in the present study on tilt-rotor aerodynamic performance.

The present neural-network-based, full-scale XV-15 tilt-rotor performance study had the following objectives:

- 1) Representation of Test Data Using Neural Networks.
  - a. Obtain neural network representations of important variables (e.g., the hover figure of merit).
  - b. Demonstrate sensitivity of selected measurements (e.g., forward flight blade bending moments) to the test parameters, such as the rotor shaft angle and advance ratio.
- 2) Assessment of Test Data Quality Using Neural Networks.
  - a. Conduct data quality checks.
  - b. Conduct quantitative error comparisons to provide an assessment of overall test data quality.
- 3) Determination of Hover Wind Corrections Using Neural-Network-Based Procedure. Formulate and implement a neural-network-based wind correction procedure for outdoor, hover performance data.

### Neural Network Approach

To accurately capture the required functional dependencies, the neural network inputs must be carefully selected and account for all important physical traits that are specific to the application. The important attributes of a neural network are its type (radial-basis function network or back-propagation network, etc.) and its complexity (i.e., the number of processing elements (PEs) and the number of hidden layers). The present overall neural network modeling approach (Refs. 1-5) consists of first determining the best type of neural network to be used and then simplifying the network as much as is practical. The latter step involves reducing the number of PEs and in a few cases, the number of hidden layers. The number of PEs required depends on the specific application. The determination of the appropriate number of PEs is done by starting with a minimum number of PEs. Additional PEs are added to improve neural network performance by reducing the RMS error between the test data and the neural network predictions. Typically, five PEs are initially added at each step in this process. Adding two or three PEs at a time "fine-tunes" the neural network.

If the correlation plot, comparing measured and predicted values, shows only small deviations from the 45 deg reference line, the neural network has produced an acceptable representation of the subject test data. If the plot shows points well off of the 45 deg line, the presence of "bad" test data is assumed. A detailed examination of the subject test

database is then required to identify the source(s) of the errors associated with these test data. As discussed under wind tunnel forward flight results, neural networks were successfully used to identify data subject to instrumentation errors. Also, the neural-network-based outdoor hover wind correction procedure illustrated herein is applied to test data with scatter. This scatter is partly due to stochastic errors, thus showing that neural networks can be applied to such real world situations.

The notation used in this paper to characterize a neural network is described as follows. A neural network architecture such as "2-5-3" refers to a neural network with two inputs, five processing elements (PEs) in the single hidden layer, and three outputs.

### Tilt-Rotor Test Database Descriptions

#### Wind tunnel hover and forward flight test database

Full-scale XV-15 tilt rotor test data for both hover and forward flight conditions (Ref. 6) were analyzed in this paper. The 25-ft diameter right hand rotor was installed on the NASA Ames Rotor Test Apparatus and tested in the NASA Ames 80- by 120-Foot Wind Tunnel. In hover, the shaft angle was varied from -15 deg to +15 deg from a vertical orientation. The relevant rotor performance variables in hover were the rotor torque coefficient,  $C_Q$ , and the figure of merit, FM. In forward flight, the lateral and longitudinal cyclic pitch, advance ratio, pitch link loads, and the blade yoke chordwise- and flatwise-bending moments are also included. These data were acquired at wind tunnel airspeeds up to 80 knots.

#### Outdoor hover test database

The full-scale outdoor XV-15 tilt-rotor hover test database was acquired as described in Refs. 7 and 8. The same rotor system was installed on the NASA Ames Propeller Test Rig and tested in propeller mode at the outdoor facility. Both axial and lateral outdoor wind measurements were taken, adding two additional variables for this problem. The outdoor XV-15 tilt-rotor hover test database included points taken with wind speeds up to 3.5 m/s. The relevant rotor hover performance variables were  $C_Q$  and FM. The present study considers hover test data with a rotor tip Mach number of 0.69 only.

### Descriptions of Outdoor Wind-Correction Hover Analyses

#### Momentum-theory-based wind correction procedure

References 7 and 8 give a wind correction procedure based on momentum theory. The momentum-theory wind corrected rotor torque coefficient  $C_{QCORRM}$  is given as follows.

$$C_{QCORRM} = C_Q + (-\mu_x C_T + \mu_y C_Y) - K(\lambda_i - \lambda_h) C_T \quad (1)$$

$$\lambda_i^2 (\mu_y^2 + (\lambda_i + \mu_x)^2) = \lambda_h^4 \quad (2)$$

Note that  $\mu_y$  (lateral wind velocity ratio) is positive in the same direction as  $C_Y$  (side force coefficient), and  $\mu_x$  (axial wind velocity ratio) is positive in the opposite direction to  $C_T$ . The parameter  $K$  is the ratio of actual induced power to ideal induced power and is assumed to be 1.16. The momentum theory corrected figures of merit data from Ref. 7 are used in this paper for comparison purposes.

#### Neural-network-based wind correction procedure

A neural network wind correction procedure was formulated and successfully implemented during the course of this study, using the outdoor

hover test data from Ref. 7. This procedure makes use of a “zero wind” neural network representation described below. This representation is based on reference variations that represent isolated rotor tilt-rotor hover performance, and which do not require any wind corrections. In the present study, the performance variables were  $C_Q$  and FM, which for the zero wind case depend only on  $C_T/\sigma$ .

In the present study, test data points with wind speeds  $<0.5$  m/s were defined to be zero wind points. The zero wind figure of merit representation, referred to as  $FM_{ZW}$ , is a function of only  $C_T/\sigma$ , and is independent of  $\mu_x$  and  $\mu_y$ . A two-hidden-layer back-propagation network with one input ( $C_T/\sigma$ ) and three outputs ( $\Theta_0$ ,  $C_Q$ , and FM) was used in the present study to obtain  $FM_{ZW}$ . The present study considers wind corrections only to the figure of merit. Details on the training of the above back-propagation network are given in the Results section.

Using the test figure of merit,  $FM_{TEST}(C_T/\sigma, \mu_x, \mu_y)$ , and the zero wind figure of merit neural network representation,  $FM_{ZW}(C_T/\sigma)$ , the variations between these two,  $\Delta_T(C_T/\sigma, \mu_x, \mu_y)$ , were formulated as follows:

$$\Delta_T(C_T/\sigma, \mu_x, \mu_y) = FM_{TEST}(C_T/\sigma, \mu_x, \mu_y) - FM_{ZW}(C_T/\sigma) \quad (3)$$

A two-hidden-layer back-propagation network with three inputs ( $C_T/\sigma$ ,  $\mu_x$ , and  $\mu_y$ ), and one output ( $\Delta_T$ ) was trained in order to predict this variation. Details on the training of this neural network are also given in the Results section. The *neural-network-predicted* variations are referred to as  $\Delta_{TNN}(C_T/\sigma, \mu_x, \mu_y)$  and represent the necessary wind corrections to yield the isolated rotor zero wind hover performance,  $FM_{CORRNN}(C_T/\sigma, \mu_x, \mu_y)$ , obtained from the following equation:

$$FM_{CORRNN}(C_T/\sigma, \mu_x, \mu_y) = FM_{TEST}(C_T/\sigma, \mu_x, \mu_y) - \Delta_{TNN}(C_T/\sigma, \mu_x, \mu_y) \quad (4)$$

**Results**

The application of neural networks to full-scale tilt-rotor hover and forward flight performance data was conducted using the neural networks package NeuralWorks Pro II/PLUS (version 5.2) by NeuralWare (Ref. 9). The present neural network RMS error was dimensionless and based on the squares of the errors for each processing element (PE) in the output layer. Generally, the RMS error was characterized by a monotonic decrease with the number of training iterations (Ref. 3). Also, any large differences in the magnitudes of the neural network variables were mitigated by appropriate scaling. In the present application, the “cost function” used in minimizing the RMS error had equally weighted individual contributions. The results from the neural network study using full-scale XV-15 tilt-rotor performance data are presented below.

**Neural-network-analysis of wind tunnel hover test data**

*Measured and derived neural network inputs.* Two back-propagation networks were trained with two different sets of inputs and outputs, shown in Table 1 as cases 1 and 2. Figures 1 and 2 show the results from two MIMO 2-5-3 back-propagation networks with inputs and outputs based on case

**Table 1. Neural network inputs and outputs**

Case	Inputs	Outputs
1.	$\Theta_0, \alpha_s$	$C_T/\sigma, C_Q, FM$
2.	$C_T/\sigma, \alpha_s$	$\Theta_0, C_Q, FM$

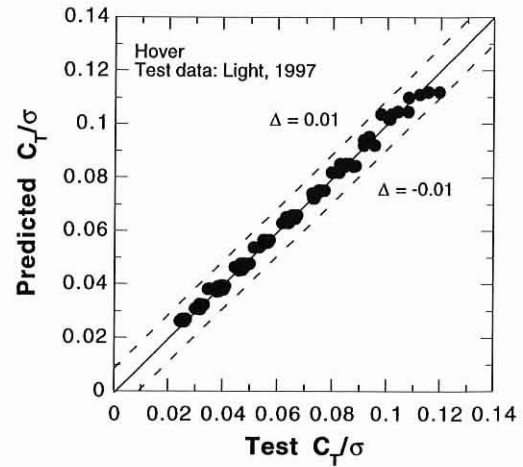


**Fig. 1. Measured inputs:  $C_T/\sigma$  correlation (MIMO 2-5-3 back-propagation neural network).**

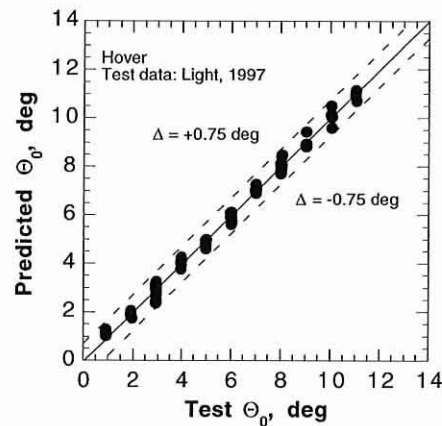


**Fig. 2. Derived inputs: collective correlation (MIMO 2-5-3 back-propagation neural network).**

1 and case 2, respectively. The neural network notation “2-5-3” refers to a network architecture with two inputs, five processing elements (PEs) in the single hidden layer, and three outputs. The MIMO 2-5-3 neural networks were both trained for 30,000 iterations with a final RMS error of 0.07 for both networks. For the case 1 data in Fig. 1, the scatter plot shows that the predicted  $C_T/\sigma$  variation clearly falls off from measured values at the highest thrust levels. For the case 2 data of Fig. 2, the scatter plot shows better agreement between predicted and test  $\Theta_0$  values. The respective error bands are shown in Figs. 1 and 2. The back-propagation network with the case 2 parameters as network inputs was judged to more accurately represent the available test data. Therefore,  $C_T/\sigma$  is used as an input parameter for all neural networks discussed below. The fidelity achieved by using  $C_T/\sigma$  as an input may be due to the high accuracy of the balance used in the Rotor Test Apparatus.

*Figure of merit versus  $C_T/\sigma$  variation.* The available test data (Ref. 6) consisted of figure of merit values for a range of  $C_T/\sigma$ 's from approximately 0.02 to 0.12 for three shaft angle values:  $-15$  deg,  $0$  deg, and  $+15$  deg. Figure 3 shows the results of three SISO 1-2-3-1 back-propagation neural network fits, where the network input was  $C_T/\sigma$  and the network output was the figure of merit. Each neural network is for a single shaft angle. Each of the three back-propagation networks was trained for 20,000 iterations with a final RMS error of 0.02 for all three

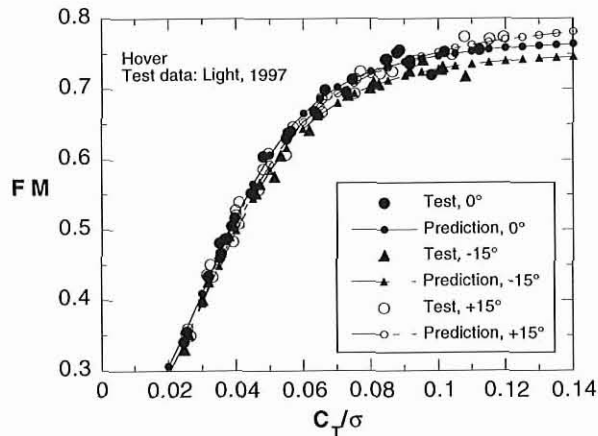


Fig. 3. Figure of merit variation with  $C_T/\sigma$ : 3 SISO 1-2-3-1 back-propagation neural network fits.

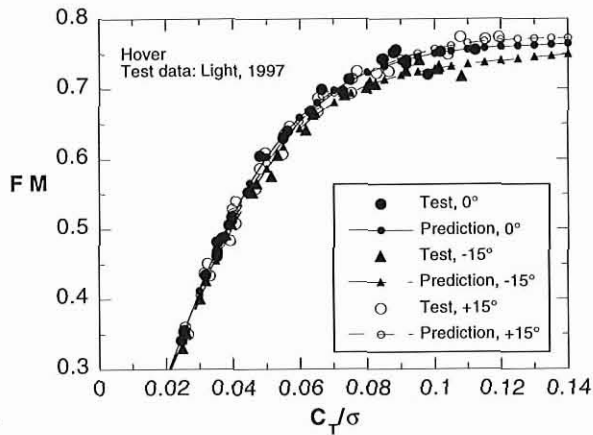


Fig. 4. Figure of merit variation with  $C_T/\sigma$ : MIMO 2-25-10-3 back-propagation neural network fit.

networks. The decrease in the test figure of merit with thrust at very high values of thrust is basically due to rotor blade stall. The neural-network-based figure of merit representations of Fig. 3 did not capture such rotor stall effects for this wind tunnel database. Reasons for this discrepancy are not known. In general, neural network theory does not guarantee an adequate means for extrapolation. Thus, each application should be considered individually. Successful extrapolation can only be obtained when the extrapolated region is reasonably close to the last data points. Also, whether an extrapolation is valid can be determined by additional testing involving expanded data domains.

Figure 4 shows the result of a single MIMO 2-25-10-3 back-propagation neural network fit, where the network inputs were both  $C_T/\sigma$  and  $\alpha_s$  and the network outputs were  $\Theta_0$ ,  $C_Q$ , and  $FM$ . The back-propagation network was trained for 34,000 iterations with a final RMS error of 0.02. Both global and more subtle effects are captured by this relatively complex 2-25-10-3 back-propagation neural network. The sensitivity of the figure of merit to the shaft angle is captured for the range of test thrust levels. However, similar to the above SISO application, the neural-network-based figure of merit representations did not fully capture rotor stall effects. The advantage of the MIMO representation is that all test conditions can be included as inputs to a single neural network, leading to improved accuracy. In fact, the MIMO neural network representations from Fig. 4 provide almost level extrapolations in the  $C_T/\sigma$  range between

0.12 and 0.14. This is an improvement over the SISO trends shown in Fig. 3.

#### Neural-network-analysis of wind tunnel forward flight test data

The following wind tunnel test parameters were selected as the forward flight neural network inputs:  $\alpha_s$ ,  $\mu$ , and  $C_T/\sigma$ . Depending on the forward flight application under consideration, the neural network output(s) were one of the following sets: i) the three control blade pitch angles, ii) the rotor torque coefficient, iii) the oscillatory pitch link loads, iv) the chordwise blade yoke bending moments (mean and oscillatory), or v) the flatwise blade yoke bending moments (mean and oscillatory). The test data used in this study is from Ref. 6.

*Rotor control settings.* The measured collective variation with shaft angle is plotted in Fig. 5. Figure 6 shows the scatter plot from a MIMO 3-10-3 back-propagation neural network, where the neural network outputs were the collective, lateral and longitudinal cyclics. The back-propagation network was trained for 200,000 iterations with a final RMS error of 0.02. Similar results were achieved for the two cyclic angles (see Ref. 10). The neural-network-based representations for the three wind tunnel test controls were considered to be very good with no obvious "bad" points, indicating that the controls test data are acceptable. Thus, neural networks can be used for compact representation of test data control inputs.

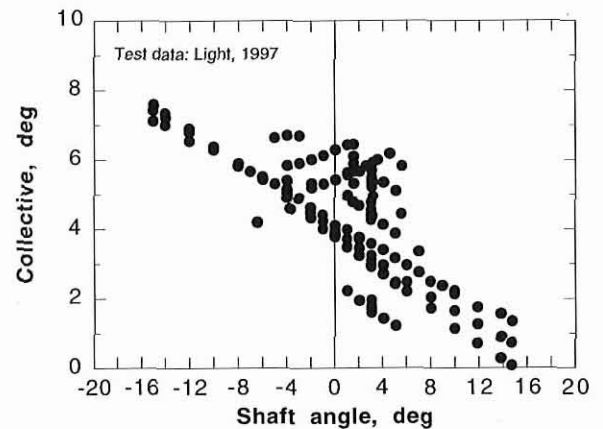


Fig. 5. Wind tunnel test data: collective versus  $\alpha_s$  (varying  $\mu$  and  $C_T/\sigma$ ), forward flight.

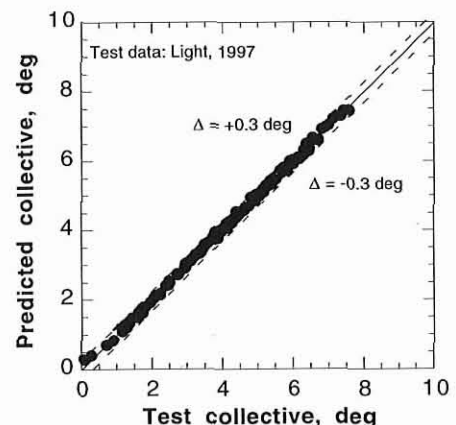


Fig. 6. Forward flight collective correlation: MIMO 3-10-3 back-propagation neural network.

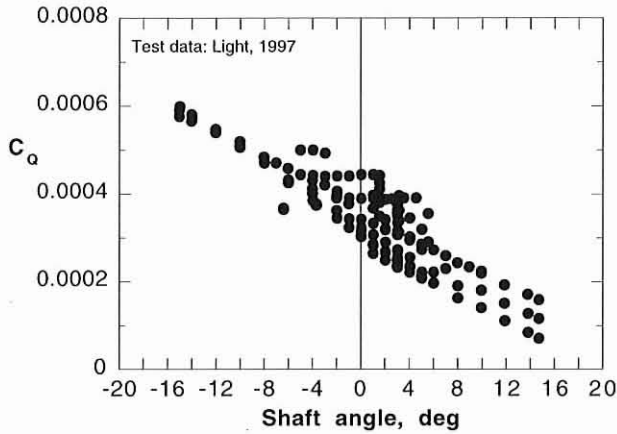


Fig. 7. Wind tunnel test data: torque coefficient versus  $\alpha_s$  (varying  $\mu$  and  $C_T/\sigma$ ), forward flight.

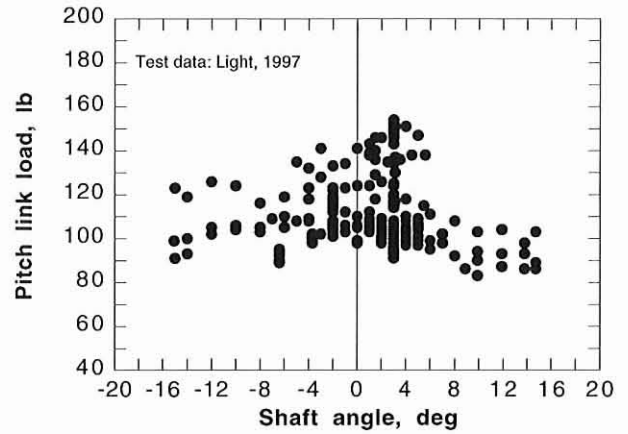


Fig. 9. Wind tunnel test data: oscillatory pitch link load versus  $\alpha_s$  (varying  $\mu$  and  $C_T/\sigma$ ), forward flight.

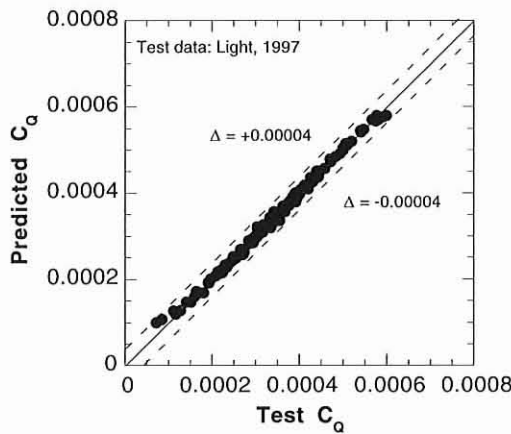


Fig. 8. Forward flight torque coefficient correlation: MIMO 3-10-1 back-propagation neural network.

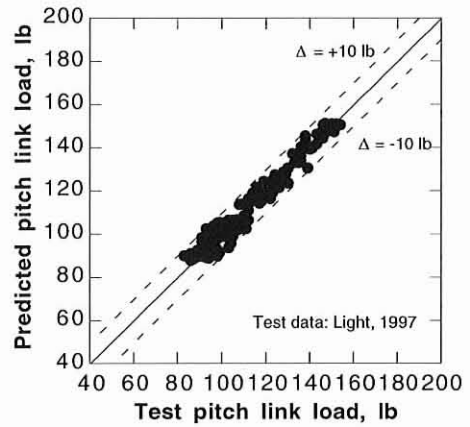


Fig. 10. Forward flight oscillatory-pitch-link-load correlation: MIMO 3-10-1 back-propagation neural network.

*Rotor torque coefficient.* The measured rotor torque coefficient variation with shaft angle is shown in Fig. 7. Figure 8 shows the scatter plot from a MISO 3-10-1 back-propagation neural network, where the neural network output was the rotor torque coefficient  $C_Q$ . The back-propagation network was trained for 100,000 iterations with a final RMS error of 0.02. The neural-network-based representation for the wind tunnel test rotor torque coefficient, Fig. 8, was considered to be very good, indicating acceptable data quality.

*Oscillatory pitch link loads.* The forward flight oscillatory test pitch link load variation with shaft angle is shown in Fig. 9. Figure 10 shows the scatter plot from a MISO 3-10-1 back-propagation neural network, where the output was the oscillatory pitch link load. The back-propagation network was trained for 200,000 iterations with a final RMS error of 0.07. The present neural-network-based representation for the oscillatory pitch link loads is within 10 lb of the correlation line, Fig. 10, which is considered to be very good. This is important in that good quality pitch link load measurements are very difficult to obtain during forward flight tests. The pitch link load database would be expected to have an inherently lower level of repeatability.

*Blade flatwise-bending moments.* The yoke flatwise mean and oscillatory bending moments for forward flight were analyzed. Figures 11 and 12 show the scatter plots from a MIMO 3-25-2 back-propagation neural network, where the neural network outputs were the mean and oscillatory

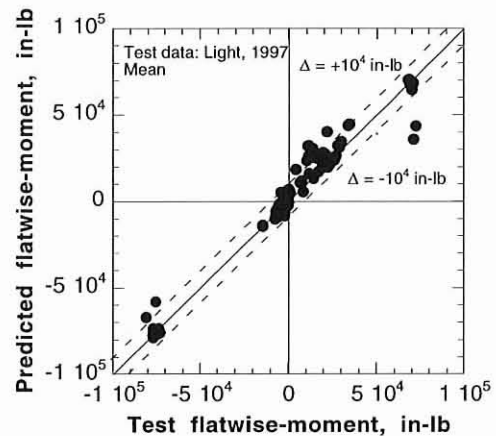


Fig. 11. Forward flight mean flatwise moment correlation: MIMO 3-25-2 back-propagation neural network.

flatwise-bending moments. The back-propagation network was trained for 200,000 iterations with an RMS error of 0.14. For data shown in Figs. 11 and 12, correlation points far away from the correlation line were judged as “bad” test data points. An examination of the flatwise-bending moment database led to the observation that some data points were not repeatable, possibly due to instrumentation problems. Indeed, the present

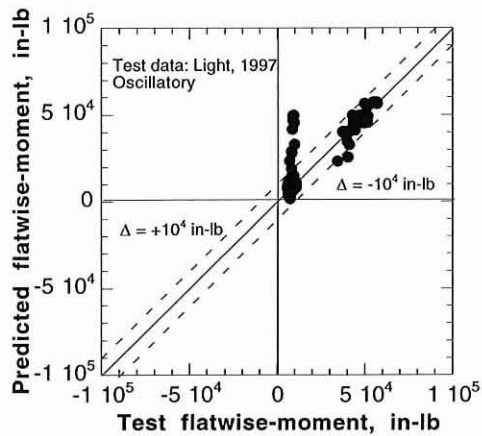


Fig. 12. Forward flight oscillatory flatwise moment correlation: MIMO 3-25-2 back-propagation neural network.

neural network analysis suggests that approximately 5% of the flatwise-bending moment database is questionable, based on the number of points outside of a  $\pm 10,000$  in-lb band. This demonstrates the ability of neural networks to indicate data of poor quality. However, the analyst should not solely rely on the neural-network-based correlation performance to eliminate test data. This process does, however, contribute to data assessment.

**Blade chordwise-bending moments.** The yoke chordwise mean and oscillatory bending moments in forward flight were considered in the neural network study. A MIMO 3-7-2 back-propagation neural network, where the neural network outputs were the mean and oscillatory chordwise-bending moments, was trained for 200,000 iterations, yielding a final RMS error of 0.02. The resulting scatter plots, which are not shown, did not indicate any "bad" points. Thus, the neural-network-based representations were considered very good for the blade yoke mean and oscillatory chordwise-bending moments and the data quality was found to be acceptable.

#### Neural-network-based, outdoor hover wind-correction procedure

**Outdoor hover test data.** The XV-15 tilt-rotor was installed with its axis oriented horizontally on the NASA Ames Propeller Test Rig and tested at this outdoor facility. Both axial and lateral wind measurements were taken, thus adding two more variables. The relevant rotor hover performance variables were  $C_T/\sigma$ ,  $\Theta_0$ ,  $C_Q$ , and FM. The hover test data is with a rotor tip mach number of 0.69. For this study, the outdoor tilt-rotor hover test database consisted of 150 data points and included data with winds up to speeds of 3.5 m/s.

**Zero wind neural network representation.** These data include points where the wind speed was less than 0.5 m/s, and included 25 test points. Figure 13 shows data for these 25 points and the resulting neural network representation derived from a SIMO 1-7-5-3 back-propagation neural network. The network input was  $C_T/\sigma$  and its three outputs were  $\Theta_0$ ,  $C_Q$ , and FM. The back-propagation network was trained for 55,000 iterations with a final RMS error of 0.02. This zero wind neural network representation for the figure of merit is referred to as  $FM_{ZW}(C_T/\sigma)$ . The non-linear stall induced characteristics are captured by the analysis.

**Figure of merit delta (FM-delta) calculation.** Figure 14 shows both the full database and the zero wind neural network representation (Fig. 13). The differences between the test data and zero wind neural network repre-

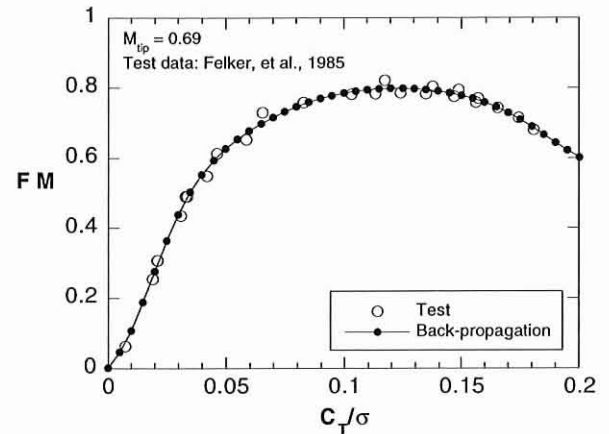


Fig. 13. Outdoor "zero wind" representation (SIMO 1-7-5-3 back-propagation neural network), winds  $< 0.5$  m/s.

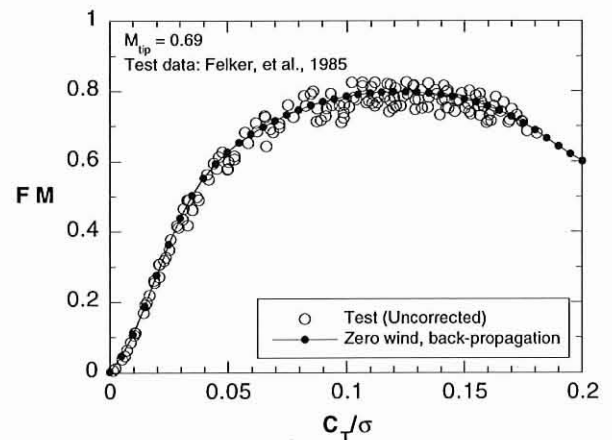


Fig. 14. Outdoor test data and zero wind curve.

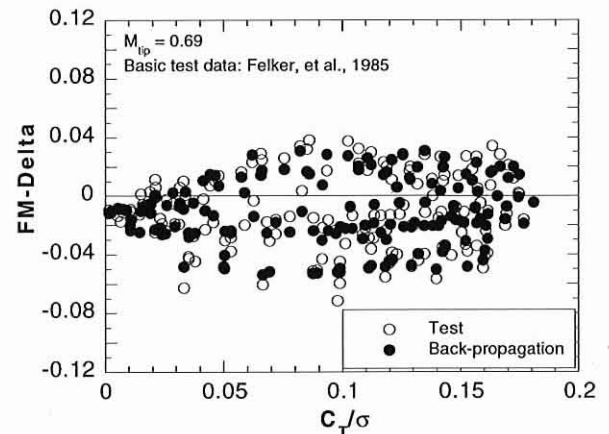


Fig. 15. Test and MISO 3-7-5-1 back-propagation neural-network-predicted figure of merit deltas ( $\Delta_T$ 's and  $\Delta_{TNN}$ 's, respectively).

sation figures of merit were calculated from Eq. 3. These differences are shown in Fig. 15 as open symbols. Neural-network-predicted differences obtained from a MISO 3-7-5-1 back-propagation network with three inputs  $C_T/\sigma$ ,  $\mu_x$ , and  $\mu_y$ , and one output  $\Delta_T$  are shown in Fig. 15 as solid circles. The back-propagation network was trained for 55,000 iterations with a final RMS error of 0.16.

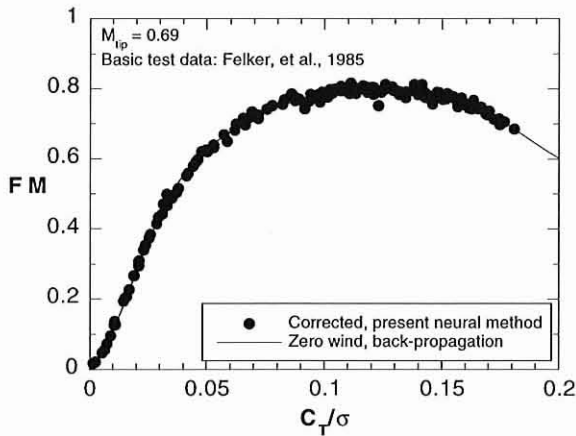


Fig. 16. Neural-network-corrected figure of merit.

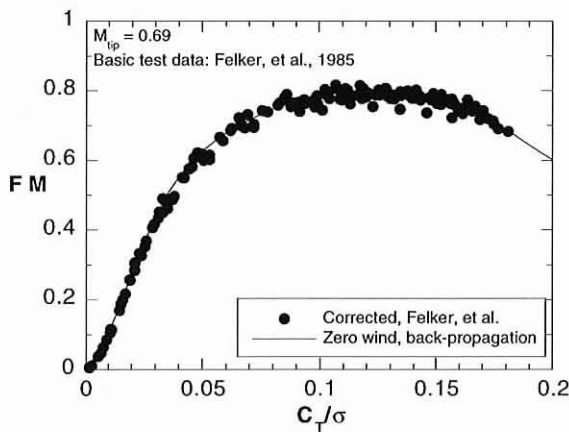


Fig. 17. Momentum-theory-corrected figure of merit (Ref. 7).

*Neural-network-corrected figure of merit.* The wind-corrected figure of merit ( $FM_{CORRNN}$ ) obtained from the present neural network approach is given by Eq. 4. Figure 16 shows the corrected figure of merit obtained from the present neural network approach and the zero wind neural network representation, illustrating that the neural-network-based wind correction procedure gives much improved results. Figure 16 also shows the worst error for a corrected data point at  $C_T/\sigma \approx 0.12$ . Subsequently, it was found that the original test data point was not valid. This was concluded by comparing the FM-deltas for data at  $C_T/\sigma \approx 0.12$  with similar wind conditions. The above noted point had an FM-delta much different from the others. Thus, in Fig. 16 the data point at  $C_T/\sigma \approx 0.12$  that stands out can be ignored and its final error does not reflect on the neural network correction procedure.

**Comparison to other figure of merit correction results**

Figure 17 shows corrected figure of merit results from Ref. 7. The present results in Fig. 16 appear more accurate with respect to scatter. The RMS errors associated with the present analysis and those of Ref. 7 were 0.01 and 0.02, respectively. This shows that corrections from the present analysis are more accurate compared to previously published results for wind corrections.

A further comparison can be made to the results from the three wind tunnel cases considered previously. The rotor shaft orientation for the outdoor case was fixed, and for this case, the above-defined error was 0.01. For the three wind tunnel cases, the rotor shaft angle was:  $-15$  deg

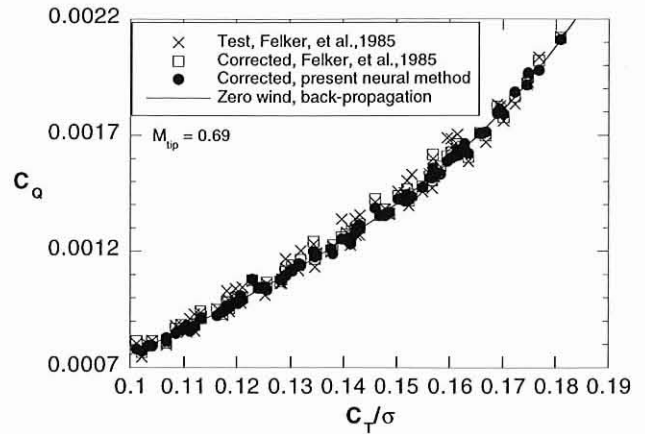


Fig. 18. Hover torque coefficient comparison, neural-network-based and momentum-theory-based.

(nose down position), 0 deg, and 15 deg. The above-defined errors for these three wind tunnel cases were: 0.05, 0.03, and 0.03, respectively. These results show that, compared to data from the wind tunnel, corrected outdoor facility data produced more accurate performance projections.

The hover rotor torque coefficients were obtained by using the following equation from Ref. 11:

$$C_Q = \frac{0.707C_T^{3/2}}{FM} \tag{5}$$

The corrected FM's have been calculated earlier in the study using a neural-networks-based wind correction procedure and also obtained from the existing, momentum-theory-based method. Figure 18 compares results from these two methods. As expected from the present figure of merit results, Fig. 18 shows that the neural-network-corrected torque coefficients were more accurate than the momentum-theory-corrected torque coefficients. The zero-wind-based RMS errors for the neural-network-based and the momentum-theory-based errors are:  $1 \times 10^{-5}$  and  $2 \times 10^{-5}$ , respectively. This again confirms that the present neural-network-based wind corrections are more accurate compared to the existing, momentum-theory-based wind corrections.

**Conclusions**

Specific conclusions from the present neural-network-based validation study on full-scale experimental tilt-rotor performance data were as follows:

- 1) Neural networks were successfully used to represent and assess the quality of tilt-rotor hover and forward flight performance and dynamic response test data.
- 2) In forward flight, measured rotor pitch settings, rotor torque, pitch link loads, and chordwise-bending moments were shown to have very acceptable data quality using neural networks. This conclusion was based on the very good correlation between the test data and the neural network predictions.
- 3) Approximately 5% of the neural network predictions of the yoke flatwise-bending moment correlated poorly with the test data. Examination of this test database showed that these test data lacked repeatability. This demonstrates that a well-trained neural network can identify data that are problematic.
- 4) Compared to existing, momentum-theory-method based wind corrections to outdoor hover performance, the neural-network-procedure corrections were better. Basically, the well-trained neural network successfully represented or mapped the test data.

### Acknowledgments

The author wishes to thank Bill Warmbrodt, Jeff Light, and Gloria Yamauchi, all of NASA Ames Research Center, for their feedback and constructive suggestions.

### References

<sup>1</sup>Kottapalli, S., "Exploratory Study on Neural Control of Rotor Noise and Hub Loads," American Helicopter Society Technical Specialists' Meeting for Rotorcraft Acoustics and Aerodynamics, Williamsburg, VA, October 28–30, 1997.

<sup>2</sup>Kottapalli, S., "Identification and Control of Rotorcraft Hub Loads Using Neural Networks," American Helicopter Society 53rd Annual Forum, Virginia Beach, VA, April 29–May 1, 1997.

<sup>3</sup>Kottapalli, S., Abrego, A., and Jacklin, S., "Application of Neural Networks to Model and Predict Rotorcraft Hub Loads," American Helicopter Society 2nd International Aeromechanics Specialists' Conference, Bridgeport, CT, October 11–13, 1995.

<sup>4</sup>Kottapalli, S., Abrego, A., and Jacklin, S., "Multiple-Input, Multiple-Output Application of Neural Networks to Model and Predict Rotorcraft Hub Loads," Sixth International Workshop on Dynamics and Aeroelas-

tic Stability of Rotorcraft Systems, Los Angeles, California, November 1995.

<sup>5</sup>Kottapalli, S., "Application of Neural Networks to Aeromechanics Problems," 24th European Rotorcraft Forum, Marseilles, France, September 15–17, 1998.

<sup>6</sup>Light, J., "Results from an XV-15 Rotor Test in the National Full-Scale Aerodynamics Complex," American Helicopter Society 53rd Annual Forum, Virginia Beach, VA, April 29–May 1, 1997.

<sup>7</sup>Felker, F. F., Betzina, M. D., and Signor, D. B., "Performance and Loads Data from a Hover Test of a Full-Scale XV-15 Rotor," NASA Technical Memorandum 86833, November 1985.

<sup>8</sup>Felker, F. F., Maisel, M. D., and Betzina, M. D., "Full-Scale Tilt-Rotor Hover Performance," *Journal of the American Helicopter Society*, Vol. 31, No. 2, April 1986, pp. 10–18.

<sup>9</sup>NeuralWorks Manuals: (a) "Reference Guide," (b) "Neural Computing," (c) "Using NeuralWorks," NeuralWare, Inc., Pittsburgh, Pennsylvania, 1995.

<sup>10</sup>Kottapalli, S., "Neural Network Research on Validating Experimental Tilt-Rotor Performance," AIAA-98-2418, 16th AIAA Applied Aerodynamic Conference, Albuquerque, New Mexico, June 1998.

<sup>11</sup>Gessow, A. and Myers, G. C., *Aerodynamics of the Helicopter*, Frederick Ungar Publishing Co., New York. Originally published in 1951 and republished in 1967.